AGU PUBLICATIONS

JGR

Journal of Geophysical Research: Oceans

RESEARCH ARTICLE

10.1002/2015JC011142

Surface gravity wave transformation across a platform coral reef in the Red Sea

S. J. Lentz[1], J. H. Churchill[1], K. A. Davis[2], and J. T. Farrar[1]

[1]Physical Oceanography, Woods Hole Oceanographic Institution, Woods Hole, Massachusetts, USA, [2]Civil and Environmental Engineering, University of California, Irvine, Irvine, California, USA

Key Points:
- Model reproduces surface gravity wave transformation across platform reef
- Dissipation dominated by bottom drag, except in narrow surf zone where wave breaking dominates
- Friction factors depend on wave orbital displacement and hydrodynamic roughness

Correspondence to:
S. J. Lentz,
slentz@whoi.edu

Citation:
Lentz, S. J., J. H. Churchill, K. A. Davis, and J. T. Farrar (2016), Surface gravity wave transformation across a platform coral reef in the Red Sea, *J. Geophys. Res. Oceans*, *121*, 693–705, doi:10.1002/2015JC011142.

Received 14 JUL 2015
Accepted 14 DEC 2015
Accepted article online 18 DEC 2015
Published online 22 JAN 2016

Abstract The transformation of surface gravity waves across a platform reef in the Red Sea is examined using 18 months of observations and a wave transformation model developed for beaches. The platform reef is 200 m across, 700 m long, and the water depth varies from 0.3 to 1.2 m. Assuming changes in wave energy flux are due to wave breaking and bottom drag dissipation, the wave transformation model with optimal parameters characterizing the wave breaking ($\gamma_m = 0.25$) and bottom drag (hydrodynamic roughness $z_o = 0.08$ m) accounts for 75%–90% of the observed wave-height variance at four sites. The observations and model indicate that wave breaking dominates the dissipation in a 20–30 m wide surf zone while bottom drag dominates the dissipation over the rest of the reef. Friction factors (drag coefficients) estimated from the observed wave energy balance range from $f_w = 0.5$ to $f_w = 5$ and increase as wave-orbital displacements decrease. The observed dependence on wave-orbital displacement is roughly consistent with extrapolation of an empirical relationship based on numerous laboratory studies of oscillatory flow. As a consequence of the dependence on wave-orbital displacement, wave friction factors vary temporally due to changes in water depth and incident wave heights, and spatially across the reef as the waves decay.

1. Introduction

Surface gravity waves impact shallow coral reefs in a number of ways. Surface waves are the dominant forcing mechanism of flow across many shallow coral reefs [*Munk and Sargent*, 1948; *Von Arx*, 1954; *Roberts et al.*, 1975; *Symonds et al.*, 1995; *Kraines et al.*, 1998; *Callaghan et al.*, 2006; *Coronado et al.*, 2007; *Jago et al.*, 2007; *Hench et al.*, 2008; *Lowe et al.*, 2009; *Vetter et al.*, 2010], including platform reefs in the Red Sea (S. Lentz, J. Churchill, K. Davis, J. Farrar, J. Pineda, and V. Starczak, The characteristics and dynamics of wave-driven flow across a platform coral reef in the Red Sea, submitted to *Journal Geophysics Research*, 2015, hereafter referred to as Lentz et al. submitted manuscript, 2015). Breaking waves at the front edge of the reef drive a setup of sea level, and the resulting pressure gradient drives flow across the reef [*Munk and Sargent*, 1948; *Monismith*, 2007; *Hearn*, 2010]. Surface waves also impact coral reef ecosystems directly by causing breakage of corals during extreme events [*Denny*, 1994; *Storlazzi et al.*, 2005] or by enhancing exchange and nutrient uptake with the surrounding water [e.g., *Falter et al.*, 2004]. A clear understanding of surface gravity wave dynamics over coral reefs is essential for developing accurate wave models. While there are well-developed and tested surface gravity wave models for continental shelves [e.g., *Booij et al.*, 1999], the usefulness of such models to estimating wave-transformations across shallow coral reefs is uncertain because of the extreme geometries and large drag that characterize reefs [*Gerritsen*, 1980; *Young*, 1989; *Lugo-Fernandez et al.*, 1998a, 1998b, *Brander et al.*, 2004; *Lowe et al.*, 2005; *Péquignet et al.*, 2011; *Harris and Vila-Concejo*, 2013; *Monismith et al.*, 2013].

The transformation of surface waves across a beach or reef is typically determined using an energy balance that assumes spatial variations in the wave-energy flux are caused by dissipation due to wave breaking ε^{wb} and bottom drag ε^{bd}, i.e.,

$$\frac{\partial(c_g E)}{\partial x} = -\varepsilon^{wb} - \varepsilon^{bd} \tag{1}$$

where c_g is the group velocity, $E = \rho g H_s^2/16$ is the wave energy, ρ is density of sea water, g is gravitational acceleration, and H_s is the significant wave height [e.g., *Battjes and Janssen*, 1978; *Thornton and Guza*, 1983; hereafter TG83].

Numerous parameterizations for wave-breaking dissipation ε^{wb} on beaches have been proposed [e.g., *Apotsos et al.*, 2008], and several have been applied to coral reefs [e.g., *Gerritsen*, 1980; *Young*, 1989; *Lowe et al.*, 2005; *Péquignet et al.*, 2011; *Filipot and Cheung*, 2012] or modified for application to coral reefs [*Massel and Gourlay*, 2000]. An evaluation of nine different parameterizations of ε^{wb} by *Apotsos et al.* [2008], found they all had similar skill in reproducing field observations of the wave transformation across beach surf zones provided an empirical parameter was tuned [see also *Filipot and Cheung*, 2012, for a similar comparison to laboratory models of coral reefs]. Based on these results, dissipation due to wave breaking is estimated here following TG83 as

$$\varepsilon^{wb} = \frac{3}{128\sqrt{2\pi}}\rho g B^3 \frac{\omega H_s^5}{\gamma_m^2 D^3}\left[1-\left\{1+\left(\frac{H_s}{\sqrt{2}\gamma_m D}\right)^2\right\}^{-\frac{5}{2}}\right], \tag{2}$$

where B is a breaker coefficient, γ_m is a model parameter related to wave-saturation in the surf zone, D is the water depth, and ω is a characteristic wave frequency. It is worth emphasizing that γ_m is simply a model parameter characterizing the wave breaking and is not the ratio of the wave height to water depth in the surf zone, even in the model. Another commonly used model [*Battjes and Janssen*, 1978] yielded similar, though slightly less accurate, estimates of the surface wave transformation across the Red Sea platform reef studied here.

For Rayleigh distributed waves, dissipation due to bottom drag is estimated as

$$\varepsilon^{bd} = \frac{\rho f_w u_w^3}{4\sqrt{\pi}} \tag{3}$$

where f_w is a wave friction factor and u_w is the near-bottom wave orbital velocity (TG83). Dissipation due to bottom drag is negligible compared to wave breaking in the surf zone over sandy beaches (TG83) but may be important over coral reefs characterized by large roughness [e.g., *Nelson*, 1996; *Lowe et al.*, 2005].

Numerous laboratory and theoretical studies indicate that the friction factor f_w depends on both the near-bottom wave orbital displacement $A_b = u_w/\omega$ and the hydrodynamic roughness z_o (or equivalent sand grain roughness $k_n = 30z_o$) [e.g., *Soulsby et al.*, 1993; *Mirfenderesk and Young*, 2003]. Laboratory studies indicate that f_w decreases from ~0.1 for $A_b/z_o = 10^2$ to less than 0.01 for $A_b/z_o = 10^5$ (Figure 1). A number of theoretical and empirical expressions have been proposed relating f_w to A_b/z_o [*Kajiura*, 1964; *Swart*, 1974; *Kamphuis*, 1975; *Jonsson and Carlsen*, 1976; *Grant and Madsen*, 1982; *Myrhaug*, 1989; *Nielsen*, 1992; *Madsen*, 1994; *Soulsby*, 1997; *Mirfenderesk and Young*, 2003]. In the range $10^2 < A_b/z_o < 10^5$, the laboratory data and the theoretical and empirical relationships are all similar. However, both the laboratory data and the various theoretical or empirical relationships diverge for $A_b/z_o < 50$ (Figure 1). For example, *Grant and Madsen* [1982] argued that for $A_b/k_n \leq 1$ ($A_b/z_o \leq 30$), $f_w = 0.23$ is a constant because "the eddy length scale will be the particle excursion rather than the bottom roughness" and some of the laboratory data seem to support a constant f_w for $A_b/z_o < 50$ [*Bagnold*, 1946; *Simons et al.*, 1988]. In contrast some of the laboratory data [*Kamphuis*, 1975; *Myrhaug et al.*, 2001] and several of the empirical relationships [e.g., *Nielsen*, 1992] suggest f_w continues to increase for $A_b/z_o < 50$.

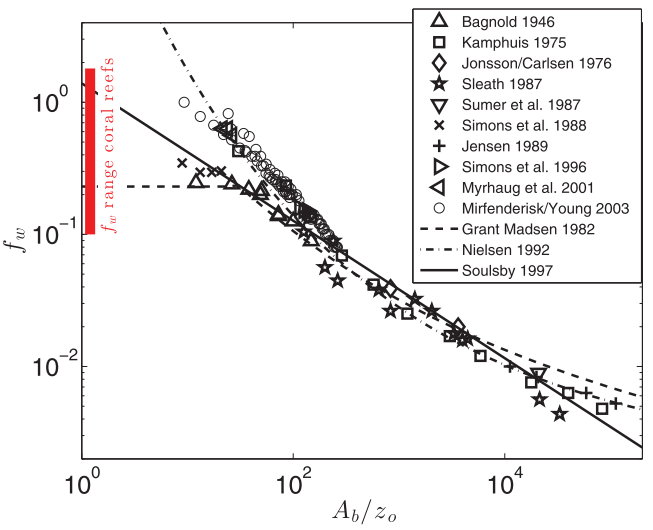

Figure 1. The dependence of wave friction factor f_w on wave orbital excursion A_b divided by hydrodynamic roughness z_o from laboratory studies (symbols; from *Soulsby et al.* [1993]; *Myrhaug et al.* [2001]; *Mirfenderesk and Young* [2003]) and examples of theoretical or empirical relationships (lines). Range of friction factor estimates for coral reefs are indicated in the top left.

The few direct estimates of friction factors over coral reefs fall in the range $f_w \approx 0.1-1.8$ [*Nelson*, 1996; *Gerritsen*, 1979; *Lowe et al.*, 2005; *Péquignet et al.*, 2011; *Huang et al.*, 2012; *Monismith et al.*, 2013; *Monismith et al.*, 2015]. Thus the coral reef friction factors are

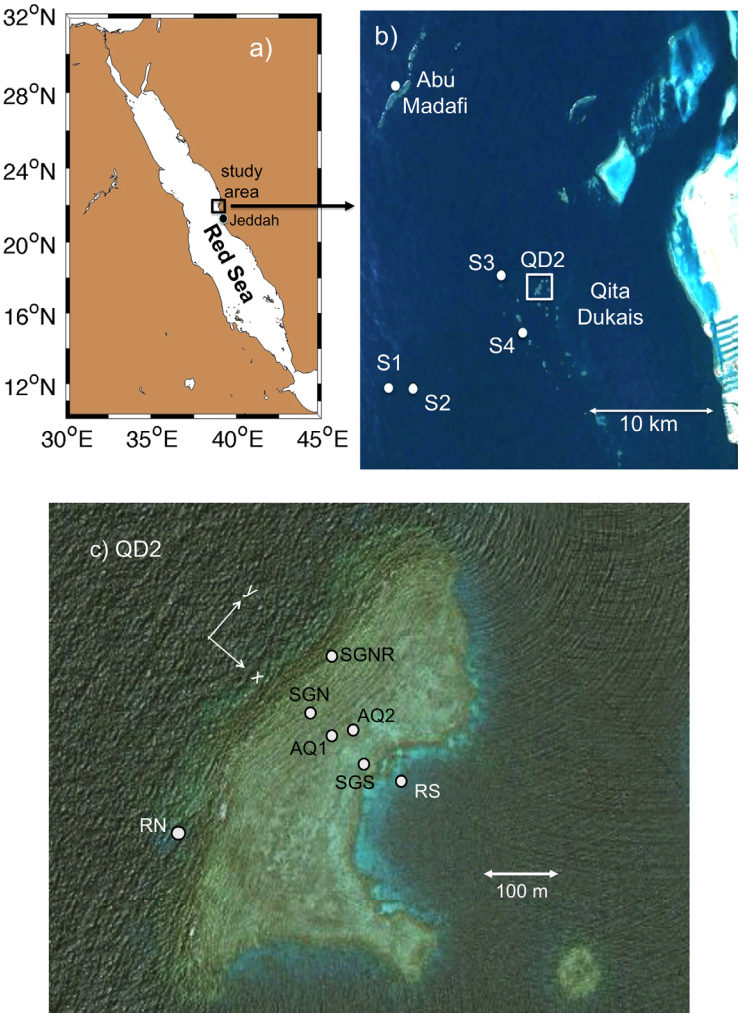

Figure 2. (a) and (b) Satellite image (Google Earth) showing coral reefs along the eastern continental shelf of the Red Sea, near Jeddah, Saudi Arabia . Wave observations were made at sites S1, S2, S3, and S4 on the shelf, and Abu Madafi at the shelf edge. The focus of this study is QD2 (c) a small reef in the Qita Dukais reef system.(c) Image of QD2 includes current profiler and pressure gauge locations. A right-handed coordinate system is adopted with *x* positive across the reef in the predominant direction of wave propagation (toward the southeast). Surface waves propagating toward QD2 break at the reef edge and then decay as they propagate across the reef.

in the range where the laboratory data and the theoretical and empirical relationships between f_w and A_b/z_o diverge (Figure 1). The coral reef studies have generally not examined the dependence of f_w on wave-orbital excursion (though see *Gerritsen* [1979]; *Rogers et al.* [2015]). Rather, an average f_w estimated from (1) is used in the empirical relationship between f_w and A_b/z_o proposed by *Nielsen* [1992] (Figure 1), or a similar expression by *Swart* [1974], to estimate a characteristic z_o (or k_n) [*Nelson*, 1996; *Lowe et al.*, 2005; *Péquignet et al.*, 2011; *Filipot and Cheung*, 2012]. For $A_b/z_o < 50$, the resulting estimates of z_o are clearly sensitive to which empirical relationship is chosen (Figure 1). To accurately estimate wave transformation across coral reefs, it is important to know how f_w depends on A_b/z_o.

Wave observations across a platform reef in the Red Sea and the wave transformation model given by (1–3) are used to examine: (1) the transformation of wave heights across the reef; (2) the relative importance of wave breaking and bottom drag to the wave transformation across the reef; (3) the accuracy of the wave transformation model; and (4) whether the friction factor f_w over this reef is constant or increases as the wave-orbital displacement decreases (Figure 1).

2. Field Site and Wave Measurements

Observations of surface gravity waves were collected over the continental shelf and several platform coral reefs on the eastern side of the Red Sea approximately 50 km northwest of Jeddah, Saudi Arabia (Figure 2a). This study focuses on the surface wave dynamics across a platform reef (QD2, our designation) in the Qita Dukais reef system (Figure 2b). QD2 is about 700 m long and 200 m across (Figure 2c). The top of the platform reef is about 1 m deep relative to mean sea level with an abrupt drop, over a horizontal distance of 1–10 m, to depths of about 15 m in the surrounding water (Figure 3). The time-averaged water depth varies across the reef platform from 0.6 m near the front (northwest side of the reef) to 1.2 m near the back (southeast side; Figure 3a). The back third of the reef contains sand channels that are 0.2–0.4 m deep (relative to the surrounding bottom), 1–2 m wide, and several meters long (Figure 3a and light colored regions in Figure 2c).

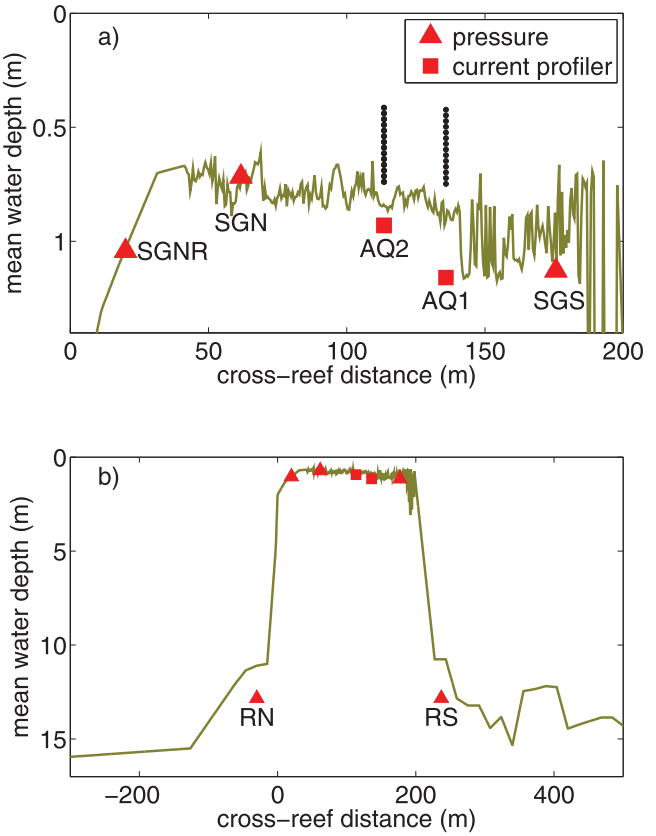

Figure 3. Bathymetry relative to mean sea level along the QD2 across-reef instrument transect (Figure 2c) (a) over the reef flat and (b) over a broader transect encompassing the platform reef. Instrument locations and heights of current profiler bins are also shown.

Surface wave observations were obtained using pressure measurements from Seabird Seagauges (SG) deployed across QD2 for three consecutive 6 month study periods: mid-November 2009 through May 2010, June through November 2010, and December 2010 through May 2011. Seagauges were deployed at SGN, ~60 m from the front edge of the reef, and SGS, ~10 m from the back edge of the reef, during all three study periods. Additionally, Seagauges were deployed at RS, behind QD2 (12 m water depth), during the first two study periods and at SGNR, at the front edge of the reef, during the third study period (Figures 2c and 3). All Seagauges collected pressure data in wave bursts at 2 Hz for 512 s every 4 h. Wave and current measurements were also obtained from an Aquadopp current profiler in pulse-coherent mode burst sampling at 1 Hz for 256 s once an hour. The Aquadopp was deployed at AQ1 during the first two 6 month study periods and at AQ2 during the third study period (Figure 2c). Spectra were computed for each wave burst and used to calculate significant wave height and peak wave period.

Surface wave observations were also obtained using RDI ADCPs deployed at shelf sites: S1, S2, and S4 from mid October 2008 to mid-November 2009; and S2, S3, and RN from mid November 2009 to early December 2010 (Figure 2b). The ADCPs collected 10 min burst samples at 2 Hz every 4 h. RDI Wavemons software was used to estimate wave directional spectra from the burst samples. The spectra were then used to estimate significant wave height, peak wave period, and wave direction. Wave observations were also collected at a meteorological buoy in the Red Sea basin approximately 40 km northwest of Qita Dukais from October 2008 to December 2010 [*Ralston et al.*, 2013] and from a Seagauge in front of Abu Madafi, a reef at the edge of the continental shelf (Figure 2b), burst sampling at 4 Hz for 512 s every 2 h from April to November 2009.

Bathymetry over the reef (Figure 3a) was measured using a downward looking Nortek Aquadopp, sampling 2-cm bins at 1 Hz, mounted under a toroid float and a handheld Garmin GPS-60 attached to a channel on top of the float. Estimates of bottom location have an accuracy of 1 cm and a horizontal resolution of about 0.2 m (the float drifted across the reef at about 0.2 m s^{-1}; see Lentz et al. submitted for details). Bathymetry was not measured near the front edge of the reef ($0 < x < 40$ m Figure 3a) using the Aquadopp because of breaking waves. Subsequently depth measurements were collected with a cross-reef resolution of about 10 m using a tape measure and handheld GPS during a period when waves were small. Bathymetry of the surrounding shelf (Figure 3b) is from a depth recorder on a small boat.

3. Results

3.1. Overview of Surface Waves Characteristics Across the Continental Shelf

Significant wave heights (H_s) in the Red Sea basin often exceed 2 m and, on one occasion, reached 4 m (Figure 4a). Peak periods are typically 4–8 s (85% of time). Significant wave heights are correlated ($r = 0.85$)

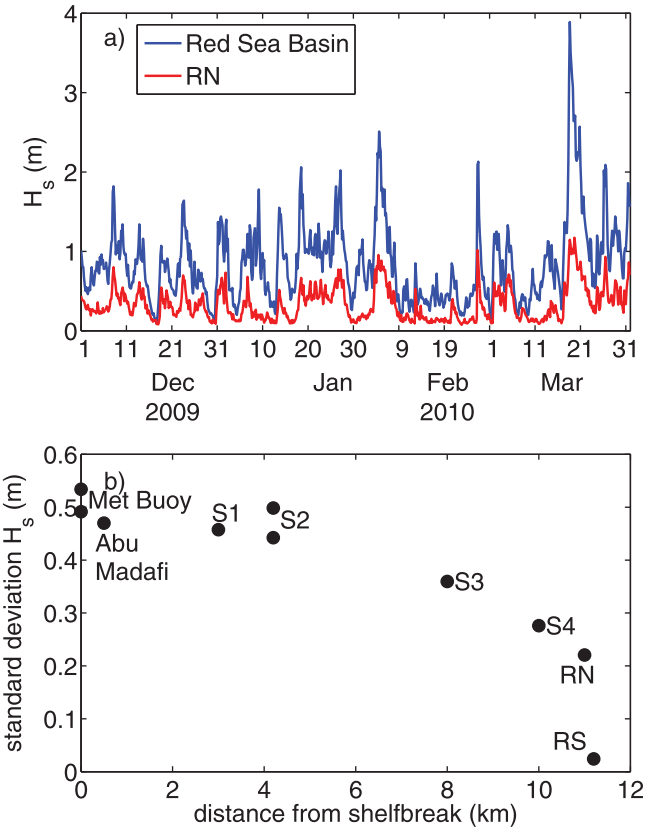

Figure 4. (a) Time series of wave height at the meteorological buoy in the Red Sea Basin (30 km offshore) and at RN in front of QD2. (b) Standard deviation of significant wave height H_s as a function of distance from the shelf edge for various sites on the continental shelf (Figure 2). RS is sheltered from the prevailing waves by QD2 (Figure 2c).

with the wind stress magnitude and waves tend to propagate southeastward along the axis of the Red Sea, in the direction of the prevailing winds [*Ralston et al.*, 2013].

Significant wave heights are highly correlated ($r > 0.9$) across the shelf. Standard deviations of H_s at the shelf-break (Abu Madafi reef) and at the outer shelf sites (S1 and S2) are similar to those at the meteorological buoy 30–35 km to the northwest (Figure 4b). However, wave heights at the Qita Dukais reef system (S4 and RN), about 10 km onshore of the continental shelf edge, are about half the wave heights at the meteorological buoy or Abu Madafi. The reduction in wave height at S3, S4, and RN relative to S1 and S2 is probably due to a combination of shadowing by Abu Madafi (Figure 2b) and dissipation associated with bottom drag. Very limited bathymetry data indicate water depths ranging from 50 to 10 m over the shelf in this region. A more detailed understanding of the processes controlling the wave height transformation across the shelf would require more accurate shelf bathymetry than is presently available and is beyond the scope of this study. At the RS site, directly behind QD2 (Figure 2c), wave heights are close to zero (Figure 4b), though the small wave heights are still significantly correlated ($r = 0.7$) with the offshore wave heights at the meteorological buoy. The following analysis is restricted to times when incident waves at RN are from the north or northwest (−65°N to 25°N), which is 87% of the times when $H_s^{RN} > 0.1$ m.

3.2. Surface Wave Transformation Across QD2: Observations

Water depths over QD2 vary substantially on annual, synoptic (days to weeks), and tidal time scales (Lentz et al. submitted manuscript, 2015). At SGN the water depth ranges from a minimum of 0.3 m to a maximum of 1.2 m, with variations of as much as 0.5 m over a few days (e.g., early February Figure 5c). Hourly burst-averaged current profiles are unidirectional and logarithmic at AQ1 and AQ2. Depth-average currents are strongly polarized cross reef with peak velocities of 0.2–0.3 m s^{-1} (Figure 5b) forced by surface gravity wave setup at the front edge of the reef. Lentz et al. (submitted manuscript, 2015) provide a detailed examination of the dynamics of the wave-driven currents across QD2.

When waves from the Red Sea basin reach the front edge of QD2 whether they break or not depends on both the incident wave height (Figure 5a, RN) and the water depth over the reef flat (Figure 5c). For moderate to large incident waves ($H_s^{RN} \geq 0.4D^{SGN}$), H_s decreases substantially from RN in front of the reef to SGN (Figures 5a and 6a symbols), presumably due to wave breaking (see section 3.4). Wave heights decay more gradually across the reef flat, from SGN to SGS (Figure 6a), presumably due to bottom drag (see section 3.4). When incident wave heights are small $\left(H_s^{RN} \leq 0.2D^{SGN}\right)$, there is not an abrupt change in wave heights at the front edge of the reef (Figure 6b symbols), presumably because the waves are not breaking. In this case, wave heights decay gradually across the reef at a rate similar to the decay behind the surf zone when waves are breaking.

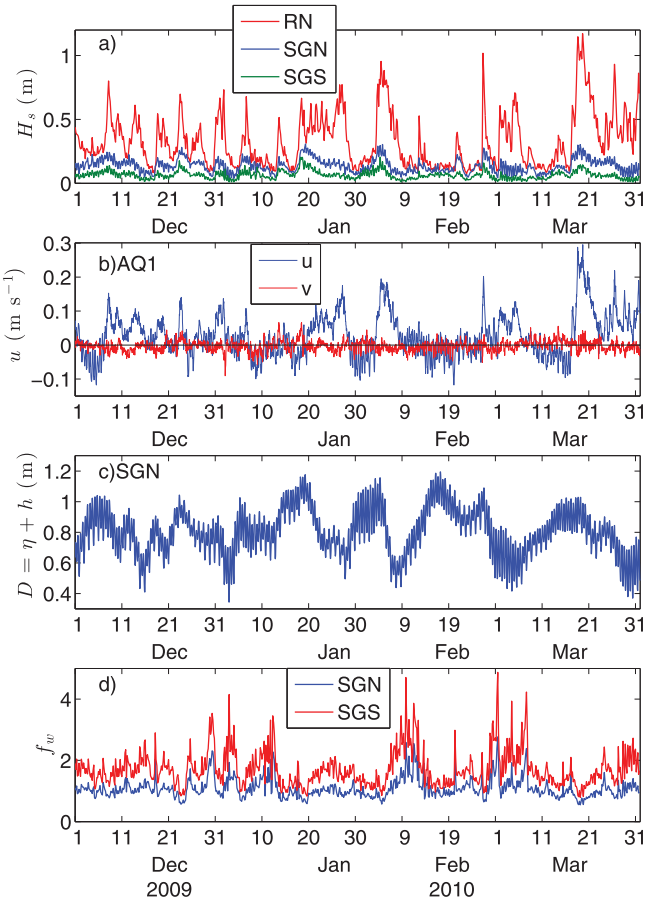

Figure 5. Time series of (a) wave heights in front of QD2 at RN and on the reef flat at SGN and SGS, (b) depth-average currents at AQ1, (c) water depth at SGN, and (d) the friction factor f_w at SGN and SGS from the wave model.

When incident wave heights are small relative to the reef water depth ($H_s^{RN} < 0.6D$ at SGNR or $H_s^{RN} < 0.3D$ at SGN Figure 7), reef wave heights increase approximately linearly with increasing incident wave height, though the wave heights over the reef tend to be smaller than the incident wave heights. When incident wave heights are larger relative to the reef water depth, wave heights over the reef are depth limited and independent of the incident wave height. A clear example of the reef flat wave height being depth limited is the period from 18 to 28 January when incident wave heights at RN are fairly constant at about 0.5 m (Figure5a), yet the wave heights over the reef flat, at SGN and SGS, decrease by a factor of two (Figure 5a) as the water depth decreases (Figure 5c). The depth limited wave heights over QD2 are qualitatively consistent with previous studies of wave breaking on both beaches and reefs [e.g., *Raubenheimer et al.*, 2001; *Lowe et al.*, 2009; *Becker et al.*, 2014]. The observations at SGNR indicate a saturation ratio of $H_s/D \approx 0.5$. However, at SGN the ratio H_s/D is smaller (0.1 to 0.3) and increases as the water depth increases because the bottom drag reduces the wave height.

To show the impact of bottom drag on H_s/D, an analytic expression for the wave height decay onshore of the surf zone is derived assuming no breaking, constant water depth, and wave friction factor, and, for convenience, shallow water waves (Appendix A). The resulting expression for the cross-reef decay of the wave height is

$$H_s(x) = \frac{\gamma D_b}{(1+(x-x_b)/L_d)} \text{ where } L_d = \frac{8\sqrt{2\pi}D_b}{f_w\gamma} \tag{4}$$

where γ is the wave height to water depth ratio at the onshore edge of the surf zone $(D=D_b,\ x=x_b)$ and L_d is a frictional decay scale. At $x-x_b=L_d$ the wave height is half the surf zone value and at $x-x_b=3L_d$ it is a quarter. Note that if $f_w=0$ then $H_s=\gamma D_b$ as expected. For $f_w=1$ and $\gamma=0.5$, $L_d \approx 40D_b$. Equation (4) accurately reproduces the observed dependence of wave height on water depth at SGN when waves are breaking $(H_s^{RN} > \gamma D_b)$ for $\gamma=0.55$ and $f_w=1.0$ (Figure 8). The agreement supports the assumption that onshore of the surf zone bottom friction modifies the relationship between wave height and water depth over the reef as indicated by (4). In particular, when bottom drag dissipation is large the ratio H_s/D is not representative of the value of $\gamma=H_s^{sz}/D^{sz}$ in the surf zone (compare red and black-dashed lines Figure 8).

3.3. Estimation of Wave Friction Factor

An estimate of the friction factor f_w is required to estimate the bottom drag dissipation and model the variation in surface wave height across QD2 using (1). Wave breaking was typically not observed onshore of SGN (e.g., Figure 2c), consistent with: the waves being depth limited in the surf zone; the water depth increasing toward the back of the reef; and bottom drag dissipation reducing the wave heights. To make an initial estimate of the friction factor, equations (1) and (3) are integrated across the reef from SGN to SGS assuming

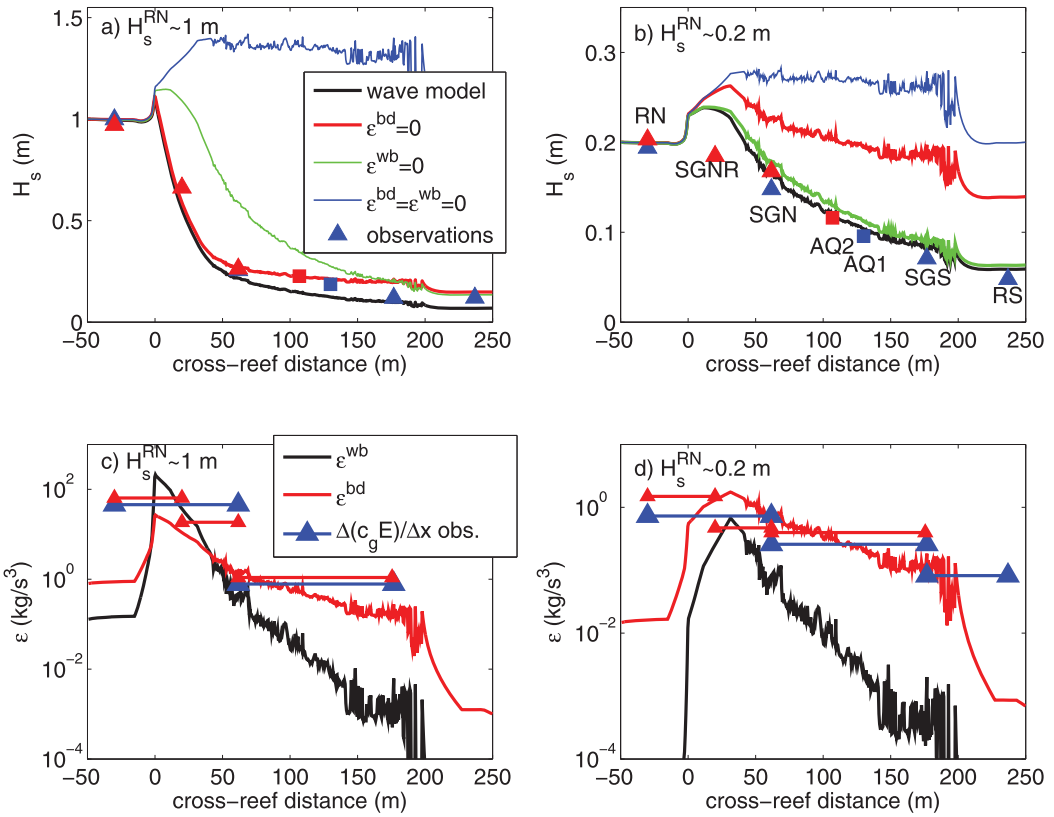

Figure 6. Significant wave heights across QD2 from observations (symbols) and the wave model (black lines) for D^{SGN}=1 m and incident waves heights of (a) H_s^{RN}=1 m and (b) H_s^{RN}=0.2 m. Figures 6c and 6d show the corresponding wave breaking ε^{wb} (black lines) and bottom drag ε^{bd} (red lines) dissipations from the model and the net dissipation estimates between sites from the observations using (1) (symbols). Symbols are mean wave heights or dissipations for all times when $0.9 < D^{SGN} < 1.1$ m and Figure 6a $0.9 < H_s^{RN} < 1.1$ m or Figure 6b $0.1 < H_s^{RN} < 0.3$ m for the first two deployments (blue) and the third deployment (red). In Figures 6a and 6b model, wave heights are also shown for no bottom drag (red), no breaking (green), and no bottom drag or breaking (blue). The front edge of reef is at 0 m and the back edge is at 200 m.

shallow water waves, ε^{wb}=0, and that both the water depth and the friction factor f_w do not vary across the reef [e.g., *Nelson*, 1996] (Appendix A). In this case,

$$f_w \approx \frac{8\sqrt{2\pi}D^2}{\Delta x}\frac{H_{SGN}-H_{SGS}}{H_{SGN}H_{SGS}} \tag{5}$$

where Δx=115 m is the distance and D is the spatially averaged water depth between SGN and SGS. To get accurate estimates of f_w, (1) should be integrated from SGN to SGS allowing for cross-reef variations in both D and f_w (section 3.4). However, (5) provides an initial determination of whether f_w depends on the wave orbital displacement A_b, as in Figure 1, independent of a particular model of that dependence. Estimates of f_w from (5) show a clear dependence on A_b, bin average values decrease from $f_w \approx 4$ for A_b=0.03 m to $f_w \approx 1$ for A_b=0.3 m (Figure 9).

To compare the QD2 estimates of f_w to the laboratory data (Figure 10) A_b is divided by the optimal hydrodynamic roughness, z_o=0.08 m, from the wave transformation model (estimated below). The QD2 estimates are at smaller values of A_b/z_o than the range of the laboratory data and are roughly consistent with extrapolation of the empirical relationship given by *Soulsby* [1997] (Figure 10, solid line). The QD2 estimates do not support the hypothesis that f_w is constant for $A_b/z_o < 50$ [*Grant and Madsen*, 1982] nor do they support the use of the steeper dependence of *Nielsen* [1992] (or similarly *Swart* [1974]) to extend the relationship to $A_b/z_o < 50$.

3.4. Wave Transformation Across QD2: Model Results

The wave transformation model described in the introduction (equations (1)–(3)) is used to determine the relative importance of wave breaking and bottom drag dissipation over the reef and to provide a more

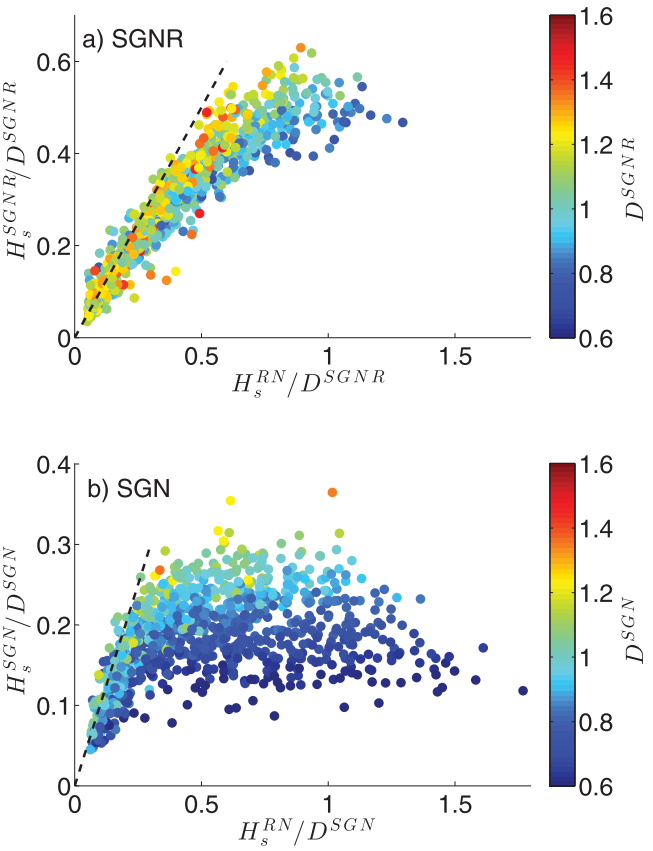

Figure 7. Significant wave height divided by water depth as a function of incident wave height divided by water depth at (a) SGNR and (b) SGN. Colors indicate water depth and dashed lines correspond to reef wave heights equaling incident wave heights.

detailed view of the cross-reef transformation of the waves. The model is one-dimensional, so it does not account for two-dimensional variability in the wave field due, for example, to along-reef variations in bathymetry and breaking or wave refraction. Visual observations at the site and the satellite image in Figure 2c suggest this is a reasonable assumption.

The abrupt change in water depth (Figure 3b), over a horizontal distance that is less than the wavelength of the incident waves (~50 m), suggests that some of the wave energy may reflect as it encounters the reef. Reflection coefficients assuming either a step or a platform geometry and ignoring breaking are ~0.6 [*Mei*, 1983]. Incorporation of a reflection coefficient in the wave transformation model had little effect on the waves over the reef because they are typically depth-limited over the shallow reef crest (Figures 7 and 8). Interestingly, directional wave spectra from RN showed no evidence of wave reflection; it is unclear why. Consequently, wave reflection is not considered in the following analysis.

To determine the optimal values of the wave-transformation model parameters, γ_m and z_o, an iterative procedure is used to minimize the root-mean-square (rms) error in the wave height estimates from (1) compared to the observed wave heights at SGN and SGS. *Apotsos et al.* [2008] set B to 1.0 because B and γ_m are not independent in most wave-transformation models [*Roelvink*, 1993]. Fitting for both γ_m and B confirmed that optimal values covaried without changing the rms error even though γ_m is independent of B in the bracket term in (2). Therefore, following *Apotsos et al.* [2008] B is set to 1. Given the incident wave height and wave period at RN, the reef bathymetry and the time-varying water depth, (1) is integrated across the reef from RN to RS at each wave-burst sample time, using (2) and (3) to estimate wave breaking and bottom-drag dissipation. The friction factor f_w is estimated using the empirical relationship given by *Soulsby* [1997] (solid line Figure 10); noting that f_w varies across the reef because it depends on the decreasing wave height and hence wave-orbital displacement A_b. The optimal wave model parameters for QD2 are z_o=0.08 m and γ_m=0.25. Optimal values determined separately for SGN and SGS and for each deployment were essentially the same (z_o=0.08±0.005, γ_m=0.25±0.03). Assuming no breaking dissipation between SGN and SGS and minimizing the rms error also yielded the same optimal value of z_o.

The wave-transformation model, with the optimal γ_m and z_o values, generally reproduces the observed wave heights at SGNR, SGN, and SGS for the observed range of incident wave characteristics and water depth variations over the reef flat (e.g., Figures 6a and 6b compare black lines and symbols). The rms error in H_s is 1.5–2.5 cm at SGN and SGS and 7 cm at SGNR. The wave model accounts for 75%–90% of the observed wave height variance (correlations 0.86–0.95) and the regression slopes are between 1.1 and 1.4 ± 0.3. The wave model estimates of dissipation also agree reasonably well with bulk estimates of the total dissipation using the observations to estimate the left-hand-side of (1) (e.g., Figures 6c and 6d compare symbols to sum of black and red lines).

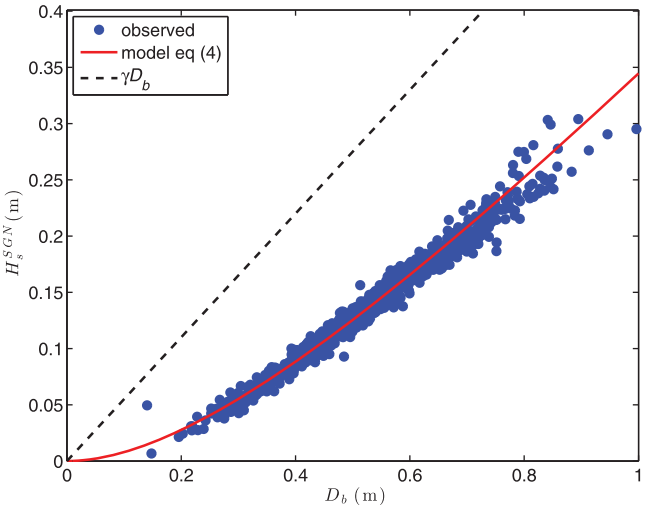

Figure 8. Comparison of the observed (blue circles) and predicted from (4) (red line) dependence of wave height on water depth at the onshore edge of the surf zone, $D_b = D^{SGN} - 0.16$ m, for times when incident waves are breaking on the reef ($H_s^{RN} > \gamma D_b$). The inferred relationship between wave height and water depth in the surf zone is also shown (dashed line). Estimates from (4) are for $\gamma = 0.55$ and $f_w = 1.0$.

The larger rms error in the model at SGNR is probably due to a number of factors, including: uncertainty in the bathymetry in the vicinity of SGNR (Figure 3) because it was in the surf zone and it was north of the instrument and bathymetry transect; SGNR being near the surf zone much of the time where there are rapid spatial variations in wave height (Figure 6a), and the larger wave heights at SGNR relative to SGN and SGS. *Péquignet et al.* [2011] also observed larger variability at a steep reef face. A robust discrepancy between the model and observations is the lack of an observed increase in wave height at SGNR relative to RN when the waves are small. In the absence of wave breaking, the model wave heights initially increase due to the decrease in water depth and conservation of wave energy flux (Figure 6b). The observations show no evidence of an increase in wave height at SGNR relative to RN (Figures 6b and 7a). This may be due to enhanced drag near the front edge of the reef and/or the uncertainty in the bathymetry at the front edge of the reef. Visual observations suggest enhanced physical roughness near the front edge of the reef suggesting that the hydrodynamic roughness is larger at SGNR than at SGN and SGS.

The wave model results indicate that in the absence of any dissipation wave heights increase over the reef because of the decrease in water depth (blue lines Figures 6a and 6b). For moderate to large waves, there is a precipitous decrease in wave height within 30–40 m of the front edge of the reef (Figure 6a) due to wave breaking (Figure 6c). Despite the large hydrodynamic roughness, bottom drag does not make a substantial contribution to the dissipation in the surf zone (Figure 6c, red line; note log scale for ε). However, the model results indicate that bottom drag dominates the dissipation from SGN (~60 m from reef edge) to the back edge of the reef (Figure 6c), though the change in wave height is small compared to the change due to wave breaking (Figure 6a, compare red and black lines). Interestingly, the bottom drag is large enough to completely damp the waves across this small platform reef (200 m) if there was no breaking (Figure 6a, green line). When the waves are small relative to the water depth, there is essentially no breaking and the dissipation is due entirely to bottom drag across the entire reef (Figures 6b and 6d). In this case, wave heights decrease by a factor of four across QD2 (Figure 6b). This transformation is consistent with previous studies of waves over reefs with less abrupt bathymetric variations [*Gerritsen*, 1980; *Young*, 1989; *Lowe et al.*, 2005;

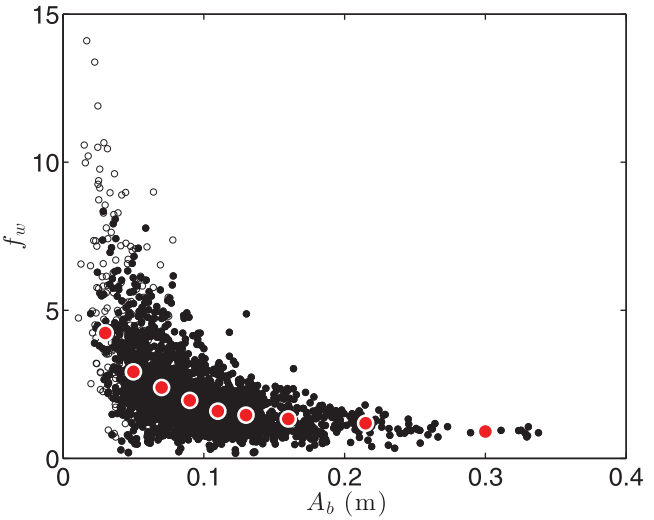

Figure 9. Bulk estimates of f_w between SGN and SGS from (5) as a function of A_b. Red circles are bin-averaged estimates of f_w. Open circles indicate $H_s < 2$ cm at SGN or SGS and are not included in bin-averages.

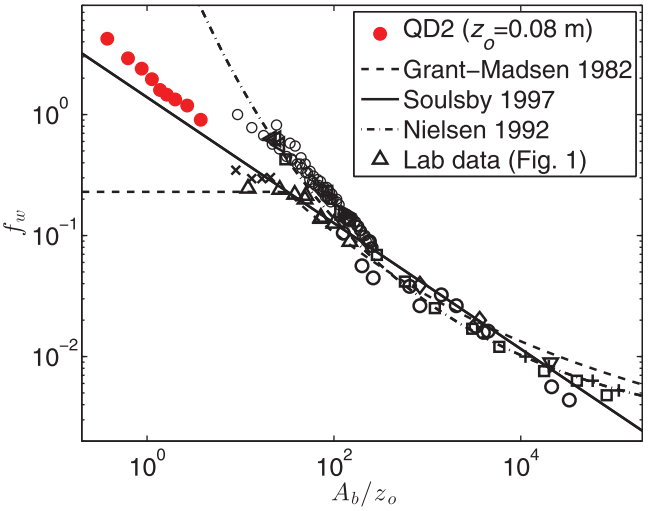

Figure 10. Bulk estimates of f_w as a function of A_b/z_o for QD2 (from Figure 8 with z_o=0.08 m) and for laboratory data (Figure 1).

Péquignet et al., 2011; *Filipot and Cheung*, 2012].

The friction factors from the model vary both temporally and spatially due to variations in wave height and wave period. The friction factor at SGN varies by a factor of three, from ~0.7 when wave heights are relatively large to ~4 when wave heights are small (Figure 5d). Since wave heights depend on water depth over the reef (Figure 8), friction factors tend to be larger when the water is shallower (compare Figures 5c and 5d). Friction factors also increase across the reef by a factor of 2–3 (compare SGN and SGS Figure 5d) because the wave height, and hence the orbital displacement, decreases across the reef (e.g., Figures 6a and 6b).

4. Discussion

The estimate of the wave-breaking parameter γ_m=0.25 from the wave transformation model is smaller than the value 0.60 (γ_{rms}=0.42) used by TG83, but closer to the tuned values (~0.4) found by *Apotsos et al.* [2008] for six studies of sandy beaches. As noted by *Apotsos et al.* [2008], the model parameter γ_m is not necessarily related to the wave saturation ratio in the surf zone $\gamma=H_s^{sz}/D^{sz}$ because B is set to 1.0 in fitting for γ_m. Direct estimates of γ from the model surf zone are ~0.5, similar to the value inferred from the SGNR observations (Figure 7a) or from fitting (4) to the SGN observations (γ=0.55, section 3.2). *Raubenheimer et al.* [1996] found empirically that over sand beaches γ increased approximately linearly with beach slope α, i.e., $\gamma \approx 0.2+6\alpha$. The observed $\gamma \approx 0.5$ at SGNR (Figure 7) is larger than predicted by this relationship, γ=0.32 for $\alpha \approx 0.02$. The observed γ for QD2 is also larger than previously observed on several coral reefs γ=0.2−0.3 [*Young*, 1989; *Brander et al.*, 2004; *Lowe et al.*, 2009; *Harris and Vila-Concejo*, 2013; *Becker et al.*, 2014]. Whether this is due to different reef geometries or under prediction of γ due to bottom drag dissipation for sites onshore of the surf zone (Figures 7b and 8) is unclear.

The estimates of f_w for QD2, ranging from 0.5 to 5 (Figures 5c and 9), are larger than estimates other most coral reefs (f_w ranging from 0.1 to 0.7) [*Nelson*, 1996; *Gerritsen*, 1979; *Lowe et al.*, 2005; *Péquignet et al.*, 2011; *Huang et al.*, 2012; *Monismith et al.*, 2013], though a recent study estimated $f_w \approx 1.8$ on the fore reef of Palmyra Atoll [*Monismith et al.*, 2015]. The relatively high values of f_w for QD2 suggest that either the hydrodynamic roughness z_o is larger and/or the wave-orbital displacements A_b are smaller than in most of the previous coral reef studies. The optimal z_o=0.08 m for QD2 from the wave model is larger than previous estimates, but all the field estimates of z_o for waves, including QD2, depend on the choice of the empirical relationship between f_w and A_b/z_o. Additionally, estimates of z_o from an average A_b and f_w, as in previous studies, are inaccurate because the relationship between f_w and A_b/z_o is nonlinear. For QD2, z_o estimated using the *Soulsby* [1997] empirical relationship and the average A_b and f_w is less than half the optimal estimate. The wave estimate of z_o=0.08 m is close to an estimate for hourly currents over QD2, z_o=0.06 m, determined by minimizing the root-mean-square difference between the bottom stress and the other terms (primarily the pressure gradient) in the depth-average cross-reef momentum balance (*Lentz et al.* submitted manuscript, 2015).

Physical roughness heights between SGN and SGS from the bathymetry survey (Figure 3a) range from 0.1 to 0.4 m, with a standard deviation of σ_r=0.13 m, similar to other coral reef flats [*Nunes and Pawlak*, 2008; *Péquignet et al.*, 2011; *Jaramillo and Pawlak*, 2011; *Huang et al.*, 2012]. The ratio of wave hydrodynamic roughness to physical roughness is $z_o/\sigma_r \approx 0.6$. This is four times larger than the ratio $z_o/\sigma_r \approx 0.15$ estimated by *Lowe et al.* [2005] for the barrier reef at Kaneohe Bay. *Huang et al.* [2012] found that $z_o/\sigma_r \approx 0.27$

provided accurate estimates of dissipation in a reef lagoon. Engineering and atmospheric boundary layer studies suggest the hydrodynamic to physical roughness ratio can range from 0.01 to 0.4 depending on, for example, the ratio of roughness frontal area to bed area [e.g., *Raupach et al*., 1991; *Britter and Hanna*, 2003; *Jimenez*, 2004].

A limitation of this analysis is that the estimated z_o is a characteristic hydrodynamic roughness for the region between SGN and SGS. Spatial variations in the physical roughness between SGN and SGS (Figure 3a) suggest there are spatial variations z_o that are not resolved by this bulk analysis.

The observations from QD2 extend the relationship between f_w and A_b/z_o to smaller values of A_b/z_o (larger f_w) than previously spanned by the laboratory studies of oscillatory flows. The QD2 results suggest that for $A_b/z_o < 50$, f_w does not increase as rapidly as suggested by *Nielsen* [1992] and others, but also is not independent of A_b/z_o as suggested by *Grant and Madsen* [1982] and others. The QD2 coral reef observations also suggest the laboratory results are relevant to geophysical scales. Evaluating the relevance of the laboratory results to surface waves over shelves and beaches has proved challenging because bottom drag dissipation is generally small relative to other processes and there is the added complexity associated with moveable beds and evolving bed forms for sand or sediment, though see *Herbers et al*. [2000] and subsequent papers. In this context, coral reefs are an ideal setting for extending and evaluating the relevance of the laboratory estimates of friction factors to geophysical flows because bottom drag dissipation is substantial.

5. Summary

The characteristics and dynamics of surface gravity waves over a ~1 m deep, 200 m wide platform reef in the Red Sea are examined using eighteen months of observations combined with a wave transformation model. The model includes a breaking parameterization developed for beaches [*Thornton and Guza* 1983] and assumes that the friction factor in the bottom drag dissipation depends on both hydrodynamic roughness and wave-orbital displacement following the empirical relationship of *Soulsby* [1997]. Optimal values of the model parameters characterizing the breaking $\gamma_m = 0.25$ and the hydrodynamic roughness $z_o = 0.08$ m were determined by minimizing the rms difference between the model and observed wave height time series. The wave model accounts for 75%–90% of the observed wave height variance.

Spatially averaged wave friction factors (drag coefficients) f_w are estimated from the observations by assuming changes in wave energy flux are due to bottom drag dissipation over the region where the waves decay gradually (i.e., where waves are not breaking). The estimated friction factors range from 0.5 to 5 and depend strongly on the wave orbital A_b displacement such that shorter wave orbital displacements result in a larger friction factor. The dependence of the friction factor on wave-orbital displacement is roughly consistent with extrapolation of an empirical relationship proposed by *Soulsby* [1997] based on numerous laboratory studies of oscillatory flow. The dependence of friction factors on orbital displacement implies that friction factors vary both temporally due to changes in water depth and incident wave heights, and spatially across the reef as the waves decay. Determining the appropriate relationship between f_w and A_b/z_o is critical to developing accurate numerical wave models for shallow coral reefs.

The wave transformation across the platform reef depends on both the incident wave height and the water depth over the reef. When incident wave heights are 40% or more of the reef water depth, waves break at the front edge of the reef and then decay more gradually across the reef flat. When incident wave heights are less than 20% of the reef-flat water depth, waves do not break but still decay gradually across the reef. The observations and the model indicate that wave breaking dominates the dissipation relative to bottom drag in a narrow (30–40 m wide) surf zone despite the large friction factors and bottom drag dominates the dissipation over the rest of the platform reef.

Appendix A

Assume a platform reef where wave height is set by wave-breaking at the shoreward edge of the surf zone $x = x_b$, so $H_s(x = x_b) = H_{sb} = \gamma D_b$ where γ is a wave saturation constant for the surf zone and $D_b = D(x = x_b)$. Further assume that onshore of the surf zone the waves only decay due to bottom dissipation (no further breaking $\varepsilon^{wb} = 0$ or change in water depth $D = D_b$), f_w is constant, and for simplicity shallow water waves over the reef flat,

$$c_g = c = \sqrt{gD},\ E = \frac{\rho g H_s^2}{16},\ \text{and}\ u_w = \frac{c}{2\sqrt{2}}\frac{H_s}{D}. \tag{A1}$$

With these assumptions and using (3) to estimate bottom dissipation, (1) reduces to

$$c_g \frac{\rho g}{16}\frac{\partial H_s^2}{\partial x} = -\frac{\rho f_w}{4\sqrt{\pi}}\left(\frac{c^3 H_s^3}{16\sqrt{2}D_b^3}\right) \rightarrow \frac{\partial H_s}{\partial x} = -\frac{f_w}{8\sqrt{2\pi}}\frac{H_s^2}{D_b^2}. \tag{A2}$$

Integrating (A2) from the shoreward edge of the surf zone x_b to some x yields

$$H_s(x) = \frac{H_{sb}}{1+\frac{f_w H_{sb}(x-x_b)}{8\sqrt{2\pi}D_b^2}} = \frac{\gamma D_b}{1+\frac{f_w \gamma (x-x_b)}{8\sqrt{2\pi}D_b}}. \tag{A3}$$

The nondimensional form of (A3) can be written as

$$\frac{H_s(x)}{H_{sb}} = \left(1+\frac{(x-x_b)}{L_d}\right)^{-1} \text{where}\ L_d = \frac{8\sqrt{2\pi}D_b}{f_w \gamma} \tag{A4}$$

is a frictional decay length scale for the reef. It is straightforward to not assume shallow water waves provided the water depth is constant. The average friction factor f_w between two sites can be estimated by integrating (A2) between the sites [*Nelson*, 1996]

$$f_w \approx \frac{8\sqrt{2\pi}D_b^2}{\Delta x}\frac{H_{s1}-H_{s2}}{H_{s1}H_{s2}}. \tag{A5}$$

Equation (A5) provides a more accurate estimate of f_w than a finite difference estimate of (1) which underestimates f_w because the bottom drag dissipation is not linear between sites.

Acknowledgments

The authors would like to thank Yasser Abualnaja, Abdulaziz Al-Suwailem, Haitham Aljahdali, Mohsen Aljahdali, Ramzi Aljahdali, Wael Almoazen, Captain Evangelos G. Aravantinos, Yasser Kattan, and all the whaler crew from King Abdullah University of Sciences and Technology (KAUST) for providing logistical and field support. We would also like to thank C. Marquette, J. Kemp, J. Ryder, S. Whelan, J. Smith, P. Bouchard, J. Lord, and the rigging shop, all of Woods Hole Oceanographic Institution (WHOI), for their efforts in instrument preparation, deployment, and recovery. This research is based on work supported by Award USA 00002 and KSA 00011 made by King Abdullah University of Science and Technology (KAUST). K. Davis was supported by a WHOI Postdoctoral Fellowship. T. Farrar was partly supported by NSF grant OCE-1435665. S. Lentz was partly supported by NSF grants OCE-1332646 and OCE-1357290. Data are available from corresponding author (slentz@whoi.edu) upon request, subject to approval from KAUST. The authors thank two anonymous reviewers for recommendations and comments that substantially improved this manuscript.

References

Apotsos, A., B. Raubenheimer, S. Elgar, and R. T. Guza (2008), Testing and calibrating parametric wave transformation models on natural beaches, *Coastal Eng.*, *55*, 224–235.

Bagnold, R. A. (1946), Motion of waves in shallow water, Interaction between waves and sand bottom, *Proc. R. Soc. London, Ser. A*, *187*, 1–15.

Battjes, J. A., and J. P. F. M. Janssen (1978), Energy loss and setup due to breaking of random waves, in *Proceedings of 16th Conference on Coastal Engineering*, pp. 569–587, Am. Soc. of Civ. Eng., N. Y.

Becker, J. M., M. A. Merrifield, and M. Ford (2014), Water level effects on breaking wave setup for Pacific Island fringing reefs, *J. Geophys. Res. Oceans*, *119*, 914–932, doi:10.1002/2013JC009373.

Booij, N., R. C. Ris, and L. H. Holthuijsen (1999), A third-generation wave model for coastal regions 1. Model description and validation, *J. Geophys. Res.*, *104*, 7649–7666, doi:10.1029/98JC02622.

Brander, R. W., P. S. Kench, and D. Hart (2004), Spatial and temporal variations in wave characteristics across a reef platform, Warraber Island, Torres Strait, Australia, *Mar. Geol.*, *207*, 169–184.

Britter, R. E. and S. R. Hanna (2003), Flow and dispersion in urban areas, *Annu. Rev. Fluid Mech.*, *35*, 469–496.

Callaghan, D. P., P. Nielsen, N. Cartwright, M. R. Gourlay, and T. E. Baldock (2006), Atoll lagoon flushing forced by waves, *Coastal Eng.*, *53*, 691–704, doi:10.1016/j.coastaleng.2006.02.006.

Coronado, C., J. Candela, R. Iglesias-Prieto, J. Sheinbaum, M. Lopez, and F. J. Ocampo-Torres (2007), On the circulation in the Puerto Morelos fringing reef lagoon, *Coral Reefs*, *26*, 149–163, doi:10.1007/s00338-006-0175-9.

Denny, M. W. (1994), Extreme drag forces and the survival of wind and water-swept organisms, *J. Exp. Biol.*, *194*, 97–115.

Falter, J. L., M. J. Atkinson, and M. A. Merrifield (2004), Mass-transfer limitation of nutrient uptake by a wave-dominated reef flat community, *Limnol. Oceanogr.*, *49*, 1820–1831.

Filipot, J.-F., and K. F. Cheung (2012), Spectral wave modeling in fringing reef environments, *Coastal Eng.*, *67*, 67–79.

Gerritsen, F. (1979), Energy dissipation in breaking waves, in *Proceedings of 5th International Conference on Port and Ocean Engineering under Arctic Conditions (POAC)*, pp. 607–619, Trondheim, POAC, Norway.

Gerritsen, F. (1980), Wave attenuation and wave set-up on a coastal reef, in *Proceedings of the 17th International Conference on Coastal Engineering*, pp. 444–461, Am. Soc. of Civ. Eng., Reston, Va.

Grant, W. D., and O. S. Madsen (1982), Movable bed roughness in unsteady oscillatory flow, *J. Geophys. Res.*, *87*, 469–481, doi:10.1029/JC087iC01p00469.

Harris, D. L., and A. Vila-Concejo (2013), Wave transformation on a coral reef rubble platform, in *Proceedings 12th International Coastal Symposium* (Plymouth, England), edited by D. C. Conley, *J. Coastal Res.*, *65*, 506–510.

Hearn, C. J. (2010), Hydrodynamics of coral reefs, in *Encyclopedia of Modern Coral Reefs*, edited by D. Hopley, pp. 563–573, Springer, Berlin.

Hench, J. L., J. J. Leichter, and S. G. Monismith (2008), Episodic circulation and exchange in a wave-driven coral reef and lagoon system, *Limnol. Oceanogr.*, *53*(6), 2681–2694, doi:10.4319/lo.2008.53.6.2681.

Herbers, T. H. C., E. J. Hendrickson, and W. C. O'Reilly (2000), Propagation of swell across a wide continental shelf, *J. Geophys. Res.*, *105*, 19,729–19,737, doi:10.1029/2000JC900085.

Huang, Z.-C., L. Lenain, W. K. Melville, J. H. Middleton, B. Reineman, N. Statom, and R. M. McCabe (2012), Dissipation of wave energy and turbulence in a shallow coral reef lagoon, *J. Geophys. Res.*, *117*, C03015, doi:10.1029/2011JC007202.

Jago, O. K., P. S. Kench, and R. W. Brander (2007), Field observations of wave-driven water-level gradients across a coral reef flat, *J. Geophys. Res.*, *112*, C06027, doi:10.1029/2006JC003740.

Jaramillo, S., and G. Pawlak (2011), AUV-based bed roughness mapping over a tropical reef, *Coral Reefs, 30*, 11–23, doi:10.1007/s00338-011-0731-9.
Jensen, B. L. (1989), Experimental investigation of turbulent oscillatory boundary layers, *Ser. Pap. 45*, Inst. Hydrodyn. and Hydr. Eng., Tech. Univ. of Denmark, Lyngby.
Jimenez, J. (2004), Turbulent flows over rough walls, *Annu. Rev. Fluid Mech.*, *36*, 173–196.
Jonsson, I. G., and N. A. Carlsen (1976), Experimental and theoretical investigations in an oscillatory turbulent boundary layer, *J. Hydraul. Res. 14*, 45–60.
Kajiura, K. (1964), On the bottom friction in an oscillatory current, *Bull. Earthquake Res. Inst. Univ. Tokyo*, *42*, 147–174.
Kamphuis, J. W. (1975), Friction factors under oscillatory waves, *J. Waterw., Harbors Coastal Eng. Div. Am. Soc. Civ. Eng.*, *101*, 135–144.
Kraines, S. B., T. Yanagi, M. Isobi, and H. Komiyama (1998), Wind-wave driven circulations on the coral reef at Bora Bay, Miyako Island, *Coral Reefs*, *17*, 133–143, doi:10.1007/s003380050107.
Lowe, R. J., J. L. Falter, M. D. Bandet, G. Pawlak, and M. J. Atkinson (2005), Spectral wave dissipation over a barrier reef, *J. Geophys. Res.*, *110*, C04001, doi:10.1029/2004.JC002711.
Lowe, R. J., J. L. Falter, S. G. Monismith, and M. J. Atkinson (2009), Wave-driven circulation of a coastal reef–lagoon system, *J. Phys. Oceanogr.*, *39*(4), 873–893, doi:10.1175/2008JPO3958.1.
Lugo-Fernandez, A., H. H. Roberts, and J. N. Suhayda (1998a), Wave transformations across a Caribbean fringing-barrier coral reef, *Cont. Shelf Res.*, *18*, 1099–1124.
Lugo-Fernandez, A., H. H. Roberts, and W. J. Wiseman (1998b), Tide effects on wave attenuation and wave setup on a Caribbean coral reef, *Estuarine Coastal Shelf Sci.*, *47*, 385–393.
Madsen, O. S. (1994), Spectral wave-current bottom boundary layer flows, in *Coastal Engineering 1994: Proceedings of the twenty-fourth International Conference*, edited by B. L. Edge, pp. 623–634, Am. Soc. Civ. Eng., Reston, Va.
Massel, S. R., and M. R. Gourlay (2000), On the modeling of wave breaking and set-up on coral reefs, *J. Coastal Eng.*, *39*, 1–27.
Mei, C. C. (1983), *The Applied Dynamics of Ocean Surface Waves*, 740 pp., John Wiley, N. Y.
Mirfenderesk, H., and I. R. Young (2003), Direct measurements of the bottom friction factor beneath surface gravity waves, *Appl. Ocean Res.*, *25*, 269–287.
Monismith, S. G. (2007), Hydrodynamics of coral reefs, *Annu. Rev. Fluid Mech.*, *39*, 37–55, doi:10.1146/annurev.fluid.38.050304.092125.
Monismith, S. G., L. M. M. Herdman, S. Ahmerkamp, J. L. Hench (2013), Wave transformation and wave-driven flow across a steep coral reef, *J. Phys. Ocean.*, *43*, 1356–1379.
Monismith, S. G., J. S. Rogers, D. Koweek, and R. B. Dunbar (2015), Frictional wave dissipation on a remarkably rough reef, *Geophys. Res. Lett.*, *42*, 4063–4071, doi:10.1002/2015GL063804.
Munk, W. H., and M. C. Sargent (1948), Adjustment of Bikini atoll to ocean waves, *Trans. AGU*, *29*, 855–60.
Myrhaug, D. (1989), A rational approach to wave friction coefficients for rough, smooth and transitional turbulent flow, *Coastal Eng.*, *13*, 11–21.
Myrhaug, D., L. E. Holmedal, R. R. Simons, and R. D. MacIver (2001), Bottom friction in random waves plus current flow, *Coastal Eng.*, *43*, 75–92.
Nelson, R. C. (1996), Hydraulic roughness of coral reef platforms, *Appl. Ocean Res.*, *18*, 265–274.
Nielsen, P. (1992), *Coastal Bottom Boundary Layers and Sediment Transport*, World Sci., Singapore.
Nunes, V., and G. Pawlak (2008), Observations of bed roughness of a coral reef, *J. Coastal Res.*, *24*, 39–50, doi:10.2112/05-0616.1.
Péquignet, A.-C., J. M. Becker, M. A. Merrifield, S. J. Boc (2011), The dissipation of wind wave energy across a fringing reef at Ipan, Guam, *Coral Reefs*, *30*, 71–82, doi:10.1007/s00338-011-0719-5.
Ralston, D. K., H. Jiang, and J. T. Farrar (2013), Waves in the Red Sea: Response to monsoonal and mountain gap winds, *Cont. Shelf Res.*, *65*, 1–13.
Raubenheimer, R., R. T. Guza, and S. Elgar (1996), Wave transformation across the inner surf zone, *J. Geophys. Res.*, *101*, 25,589–25,597, doi: 10.1029/96JC02433.
Raubenheimer, R., R. T. Guza, and S. Elgar (2001), Field observations of wave-driven setdown and setup, *J. Geophys. Res.*, *106*, 4629–4638, doi:10.1029/2000JC000572.
Raupach, M. R., R. A. Antonia, and S. Rajagopalan (1991), Rough-wall turbulent boundary layers, *Appl. Mech. Rev.*, *44*, 1–25.
Roberts, H. H., S. P. Murray, and J. H. Suhayda (1975), Physical processes in a fringing reef system, *J. Mar. Res.*, *33*, 233–260.
Roelvink, J. A. (1993), Dissipation in random wave groups incident on a beach. *Coastal Eng.*, *19*, 127–150.
Rogers, J. S., S. G. Monismith, D. A. Koweek, and R. B. Dunbar (2015), Wave dynamics of a Pacific atoll with high frictional effects, *J. Geophys. Res. Oceans*, doi:10.1002/2015JC011170.
Simons, R. R., A. Kyriacou, R. L. Soulsby, and A. G. Davies (1988), Predicting the nearbed turbulent flow in waves and currents, in *Proceedings of IAHR Symposium on Mathematical Modelling of Sediment Transport in The Coastal Zone*, pp. 33–47, International Association for Hydro-Environment Engineering and Research (IAHR), Copenhagen, Denmark.
Simons, R. R., R. D. MacIver, and W. M. Saleh (1996), Kinematics and shear stresses from combined waves and longshore currents in the UK Coastal Research Facility, in *Proceedings of 25th Conference on Coastal Engineering*, pp. 3481–3494, Am. Soc. of Civ. Eng., Orlando.
Sleath, J. F. A. (1987), Turbulent oscillatory flow over rough beds. *J. Fluid Mech.*, *182*, 369–409.
Soulsby, R. L. (1997), *Dynamics of Marine Sands: A Manual for Practical Applications*, Thomas Telford, London, U. K.
Soulsby, R. L., L. Hamm, G. Klopman, D. Myrhaug, R. R. Simons, and G. P. Thomas (1993), Wave-current interaction within and outside the bottom boundary layer, *Coastal Eng. 21*, 41–69.
Storlazzi, C. D., E. K. Brown, M. E. Field, K. Rodgers, and P. L. Jokiel (2005), A model for wave control on coral breakage and species distribution in the Hawaiian Islands, *Coral Reefs*, *24*, 43–55.
Sumer, B. M., B. L. Jensen, and J. Fredsøe (1987), Turbulence in oscillatory boundary layers, in *Advances in Turbulence*, edited by C. Comte-Bellot and E. Mathieu, pp. 556–567, Springer, Berlin.
Swart, D. H. (1974), Offshore sediment transport and equilibrium beach profiles, *Delft Hydraulics Lab. Publ*. vol. 131, Delft Hydraulics Laboratory, Delft, Netherlands.
Symonds, G., K. P. Black, and I. R. Young (1995), Wave-driven flow over shallow reefs, *J. Geophys. Res.*, *100*, 2639–2648, doi:10.1029/94JC02736.
Thornton, E. B., and R. T. Guza (1983), Transformation of wave height distribution, *J. Geophys. Res.*, *88*, 5925–5938, doi:10.1029/JC088iC10p05925.
Vetter, O., J. M. Becker, M. A. Merrifield, A.-C. Pequignet, J. Aucan, S. J. Boc, and C. E. Pollock (2010),Wave setup over a Pacific Island fringing reef, *J. Geophys. Res.*, *115*, C12066, doi:10.1029/2010JC006455.
Von Arx, W. S. (1954), Circulation systems of Bikini and Rongelap lagoons, Bikini and nearby atolls, Marshall Islands, *US Geol. Surv. Prof. Pap.*, *260-B*, 265–273.
Young, I. R. (1989), Wave transformations on coral reefs, *J. Geophys Res.*, *94*, 9979–9989, doi:10.1029/JC094iC07p09779.